OPEN

Cell Death and Differentiation (2016) 23, 89–98

www.nature.com/cdd

NF-κB pathway controls mitochondrial dynamics

M Laforge[1], V Rodrigues[1,2], R Silvestre[3], C Gautier[4,5,6], R Weil[7], O Corti[4,5,6] and J Estaquier*[,1,8]

The Optic atrophy 1 protein (OPA1) is a key element in the dynamics and morphology of mitochondria. We demonstrated that the absence of IκB kinase-α, which is a key element of the nonclassical NF-κB pathway, has an impact on the mitochondrial network morphology and OPA1 expression. In contrast, the absence of NF-κB essential modulator (NEMO) or IκB kinase-β, both of which are essential for the canonical NF-κB pathway, has no impact on mitochondrial dynamics. Whereas Parkin has been reported to positively regulate the expression of OPA1 through NEMO, herein we found that *PARK2* overexpression did not modify the expression of OPA1. *PARK2* expression reduced the levels of Bax, and it prevented stress-induced cell death only in Bak-deficient mouse embryonic fibroblast cells. Collectively, our results point out a role of the nonclassical NF-κB pathway in the regulation of mitochondrial dynamics and OPA1 expression.
Cell Death and Differentiation (2016) **23,** 89–98; doi:10.1038/cdd.2015.42; published online 29 May 2015

Mitochondria perform multiple functions that are critical to the maintenance of cellular homeostasis. Mitochondrial dysfunctions have been linked to the development of degenerative diseases and aging. Damaged mitochondria are removed by mitophagy, a process partially regulated by the *PARK2*-encoded E3 ubiquitin ligase (Parkin) in a PTEN-induced putative protein kinase 1 (PINK1)-dependent manner.[1–4] During mitophagy, the phosphorylation of mitofusin (Mfn) 2 by PINK1 has been suggested to induce the recruitment of Parkin to the mitochondria in cardiomyocytes.[5] However, previous groups have shown that that Mfn 1 and 2 are dispensable for Parkin-dependent mitophagy in fibroblasts, whereas the Parkin-dependent degradation of these proteins may impair fusion of damaged mitochondria with the healthy network.[6–8] PINK1 and Parkin thus act as a quality control machinery on the outer mitochondrial membrane (OMM) to preserve mitochondrial integrity through the ubiquitination of OMM proteins.[9,10] Moreover, through its E3 ubiquitin ligase activity,[11,12] Parkin was reported to bind to the linear ubiquitin chain assembly complex (LUBAC) and to increase the ubiquitination of NF-κB essential modulator (NEMO),[13] a component of the classical NF-κB signaling pathway.[14] Müller–Rischart *et al.* also proposed that Parkin positively regulates the expression of the mitochondrial guanosine triphosphatase Optic atrophy 1 protein (OPA1) through linear ubiquitination of NEMO.[13] OPA1 is a regulator of mitochondrial inner membrane fusion and cristae remodeling.[15–17] A defect in OPA1 expression is associated with mitochondrial network fragmentation and enhanced sensitivity of the cells to undergo apoptosis by promoting cytochrome *c* release from the mitochondria.[18–20] Because NEMO-deficient mouse embryonic fibroblast (MEF) cells display a normal mitochondrial network morphology, we decided to re-examine the role of Parkin in regulating OPA1 expression through the NF-κB signaling pathway.

Results and discussion

Overexpression of Park2 is not associated with higher levels of OPA1. On the basis of the observation that NEMO-deficient MEF cells display a mitochondrial network morphology without fragmentation (Figure 1a) and exhibit the same levels of OPA1 isoforms in comparison with wild-type (WT) MEF cells (Figure 1b), we analyzed the mitochondrial network in Parkin-deficient MEF cells (Figure 1c). Confocal microscopy revealed a decrease in the size of mitochondria, although mantaining similar numbers per cell when compared with WT MEF cells (Figures 1c–e). Previous reports from fibroblasts of patients with *PARK2* mutations showed similar degrees of branching under basal culturing conditions.[21,22] In the presence of protonophore carbonyl cyanide 3-chlorophenylhydrazone (CCCP), mitochondrial network is fragmented in Parkin-deficient cells (Figure 1d). Analysis of OPA1 expression in Parkin-deficient cells revealed a decrease of ~24% in the amount of OPA1 compared with WT cells (Figure 1f), in agreement with Müller–Rischart *et al.*[13]

To further examine the role of Parkin in OPA1 regulation, we cotransfected WT, Parkin-, and NEMO-deficient MEF cells with an expression plasmid for *PARK2* and a GFP plasmid to monitor the percentage of transfected cells. We achieved a cell transfection efficiency of ~40%, as quantified by flow

[1]CNRS FR 3636, Université Paris Descartes, Paris, France; [2]Parasite Disease Group, Instituto de Biologia Molecular e Celular, Universidade do Porto, Porto, Portugal; [3]Life and Health Sciences Research Institute (ICVS), School of Health Sciences, University of Minho; ICVS/3B's-PT Government Associate Laboratory, Braga/Guimarães, Portugal; [4]Inserm, U 1127, F-75013 Paris, France; [5]CNRS, UMR 7225, F-75013 Paris, France; [6]Sorbonne Universités, UPMC Univ Paris 06, UMR S 1127, F-75013 Paris, France; [7]Unité de Signalisation Moléculaire et Activation Cellulaire, Institut Pasteur, Unité CNRS URA 2582, Paris, France and [8]Centre de Recherche en Infectiologie, Université Laval, Québec, Canada

*Corresponding author: J Estaquier, Centre de Recherche en Infectiologie, Université Laval, Québec, Canada G1V 4G2. Tel: +418 525 44 44; E-mail: estaquier@yahoo.fr
Abbreviations: CCCP, carbonyl cyanide 3-chlorophenylhydrazone; IKKβ, IκB kinase-β; IKKα, IκB kinase-α; LUBAC, linear ubiquitin chain assembly complex; Mfn, mitofusin; OMM, outer mitochondrial membrane; MEF, mouse embryonic fibroblasts; ΔΨm, mitochondrial membrane potential; NEMO, NF-κB essential modulator; OPA1, Optic atrophy 1; PI, propidium iodide; PINK1, PTEN-induced putative protein kinase 1; STS, Staurosporine
Received 18.11.13; revised 13.1.15; accepted 27.1.15; Edited by L Scorrano; published online 29.5.15

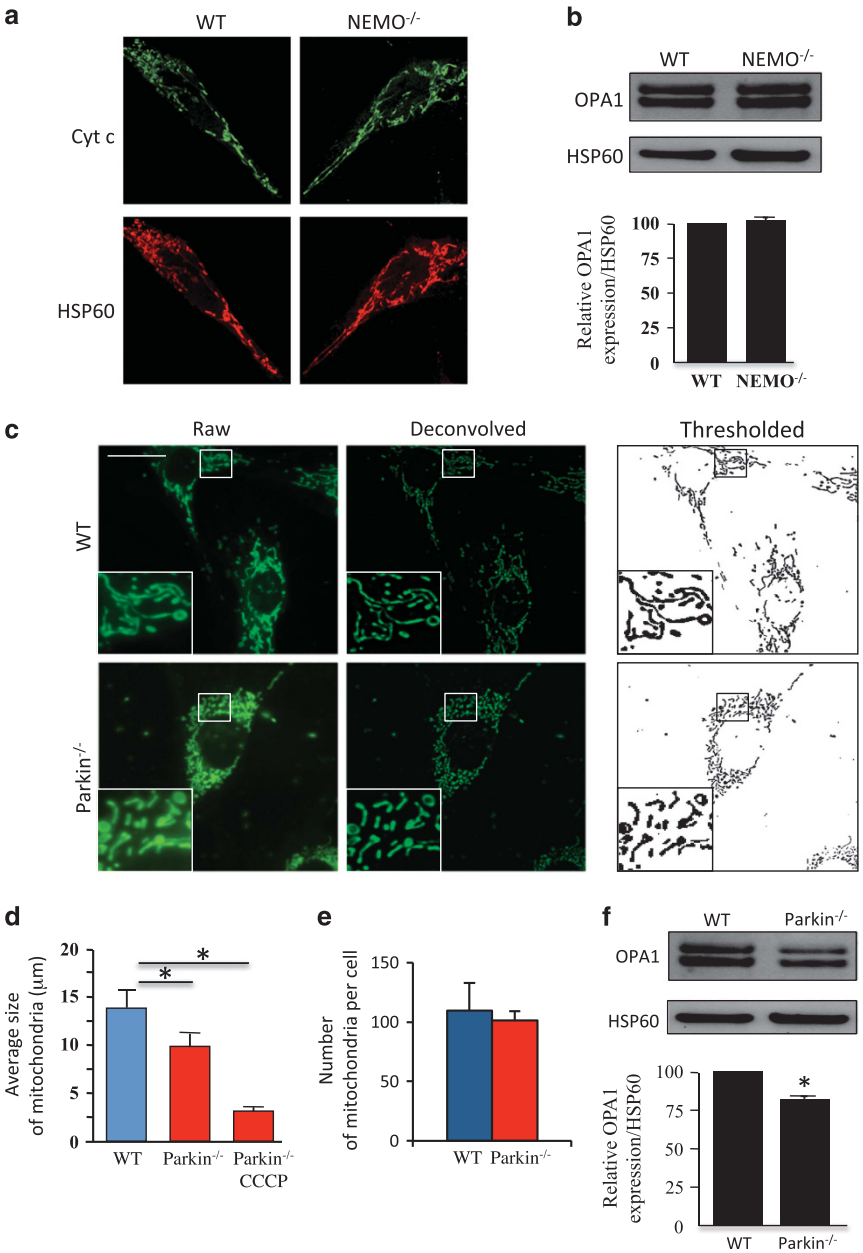

Figure 1 Mitochondrial morphology and OPA1 expression in NEMO- and Parkin-deficient MEF cells. (**a**) WT and NEMO$^{-/-}$ cells were stained with specific antibodies directed against cytochrome *c* (Cyt *c*, in green) and Hsp60 (in red). (**b**) OPA1 profile in WT and NEMO$^{-/-}$. Immunoblot was probed with specific OPA1 antibodies. Hsp60 was used as a loading control to normalize protein content. Results correspond to the mean of three experiments. (**c**) Mitochondrial network in WT and Parkin$^{-/-}$ cells. MEFs were stained with MitoTracker Green and imaged on an inverted microscope to obtain raw epifluorescence images (left panels). Deconvolved images (center panels) were obtained by subtracting a Gaussian blur (σ: 12) to the original images. Deconvolved images were then thresholded to obtain a binary image of the mitochondrial network (right panels) used for the automatized analysis of the size and the number of mitochondria in each individual cell. (**d** and **e**) Bar graphs showing (**d**) the average number and (**e**) the average size of mitochondria in WT and Parkin$^{-/-}$ MEFs in the absence or presence of CCCP ($n = 130$, 136, and 120, respectively). (**f**) OPA1 profile in WT and Parkin$^{-/-}$ MEFs. Immunoblot was probed with specific OPA1 antibodies. Hsp60 was used as a loading control to normalize protein content. Results are from three experiments, $^{*}P < 0.05$

cytometry at 24 h (Figure 2a). Parkin expression was assessed by western blotting, and actin was used as a control for loading. Analysis of OPA1 expression in *PARK2*-transfected cells did not reveal an increase in the amount of OPA1 in WT and Parkin$^{-/-}$ (Figures 2b and c). In NEMO-deficient MEFs such as WT or Parkin-deficient MEFs, the overexpression of Parkin following transfection at a dose of 1 μg of plasmid rather resulted in a decrease, although not significant, in the amount of OPA1 (Figure 2d). Because Müller–Rischart *et al.*[13] reported a significant upregulation in protein levels of OPA1, both under basal conditions and in the presence of CCCP, we treated WT- and NEMO-deficient MEF cells with CCCP (Figure 3). CCCP induced the degradation of the long isoform of OPA1 (Figures 3a and b), as previously described.[15,16,18–20] In the presence of Parkin, no difference in the levels of OPA1 was observed either at 3 or 24 h post

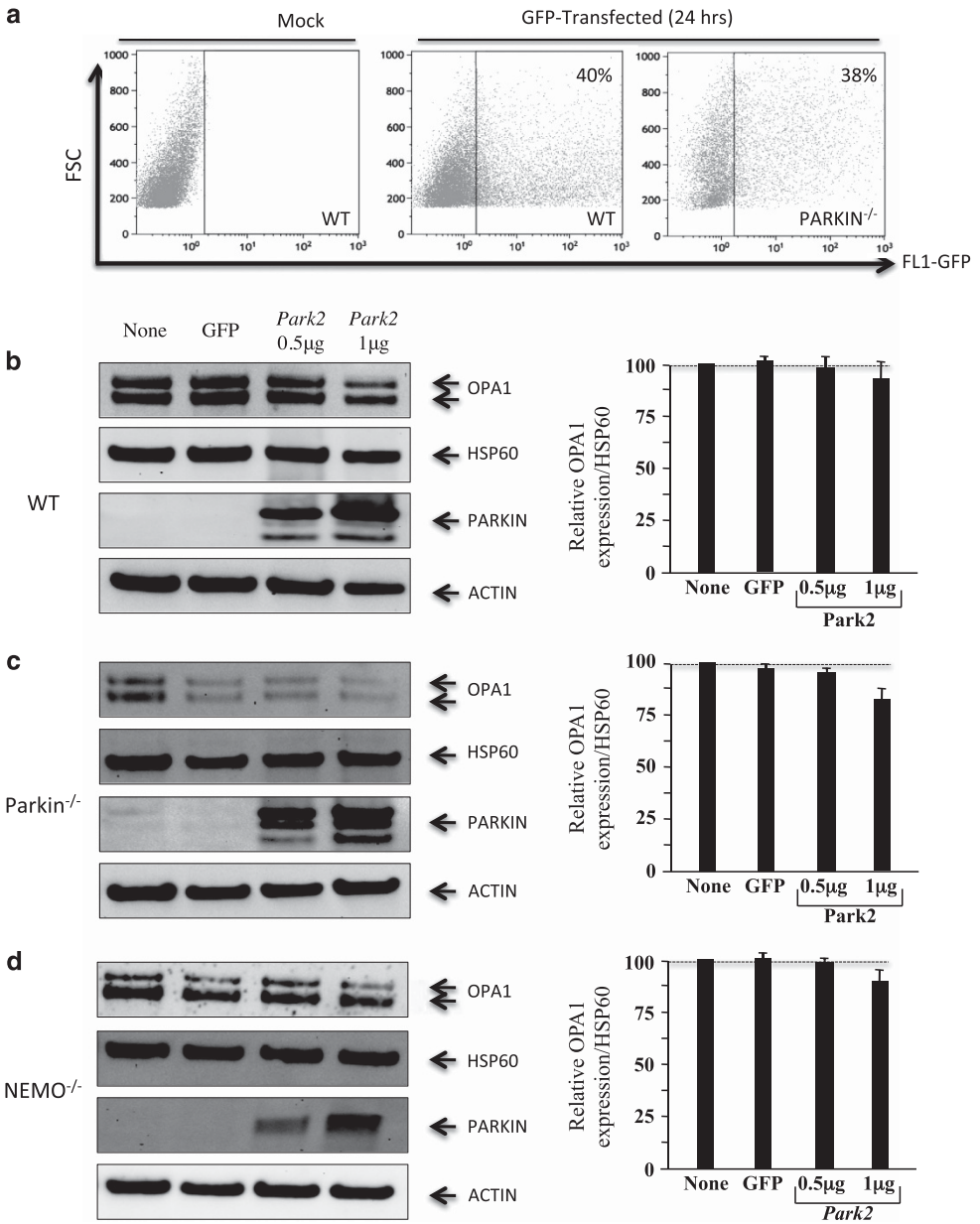

Figure 2 OPA1 protein expression in Parkin-tranfected MEF cells. (**a**) Efficiency of cell transfection. Cells were cotransfected with Parkin and GFP (1 μg) or mock. Green fluorescent intensity was determined by flow cytometry after 24 h (**b**–**d**). Profile of OPA1 expression in WT, Parkin$^{-/-}$, and NEMO$^{-/-}$ MEFs (left panels), and quantification of the amount of OPA1 isoforms (right panels). The values indicate the relative levels of the long isoforms with respect to the baseline (value 1), in the absence (none) or after 24 h of transfection with either a GFP or *PARK2* vector at the dose of 0.5 and 1 μg. HSP60 was used as a loading control to normalize protein content. Immunoblots were also probed with specific Parkin antibodies. Actin was used as a loading control. Four experiments were performed

treatment (Figures 3a and b). This result is consistent with a previous report from Lutz *et al.* showing that the absence of parkin does not alter the proteolytic processing of OPA1 in SH-SY5Y cells.[23] It has been proposed that mitochondrial fission related to Drp1 induces mitochondrial network fragmentation in Parkin-deficient cells.[23] Furthermore, in both cell lines, CCCP induced mitochondrial network fragmentation (Figures 3c and d) and dissipation of mitochondrial membrane potential (ΔΨm loss) (Figures 3e and f). Moreover, in the presence of Parkin, the mitochondrial membrane potential of CCCP-treated MEF is even reduced, suggesting a removal of damaged mitochondria (Figures 3c and f), which is consistent with previous reports on the functional role of Parkin on mitochondria.[6,7]

IKK*α*-deficient MEF cells display lower levels of OPA1 and a fragmented mitochondrial network. The NF-κB/Rel family is composed of several members, including RelA (p65), RelB, c-Rel, NF-κB1 p50, and NF-κB2 p52.[14] NF-κB proteins are regulated through their interaction with specific inhibitors, the IκB proteins (IκB*α*, IκB*β*, or IκB*ε*), which keep them in an inactive form in the cytoplasm of cells. The classical NF-κB pathway involves a huge complex containing NEMO and IκB kinase-*β* (IKK*β*), but not IκB kinase-*α* (IKK*α*). IKK*α* and IKK*β* phosphorylate IκB proteins, which trigger their

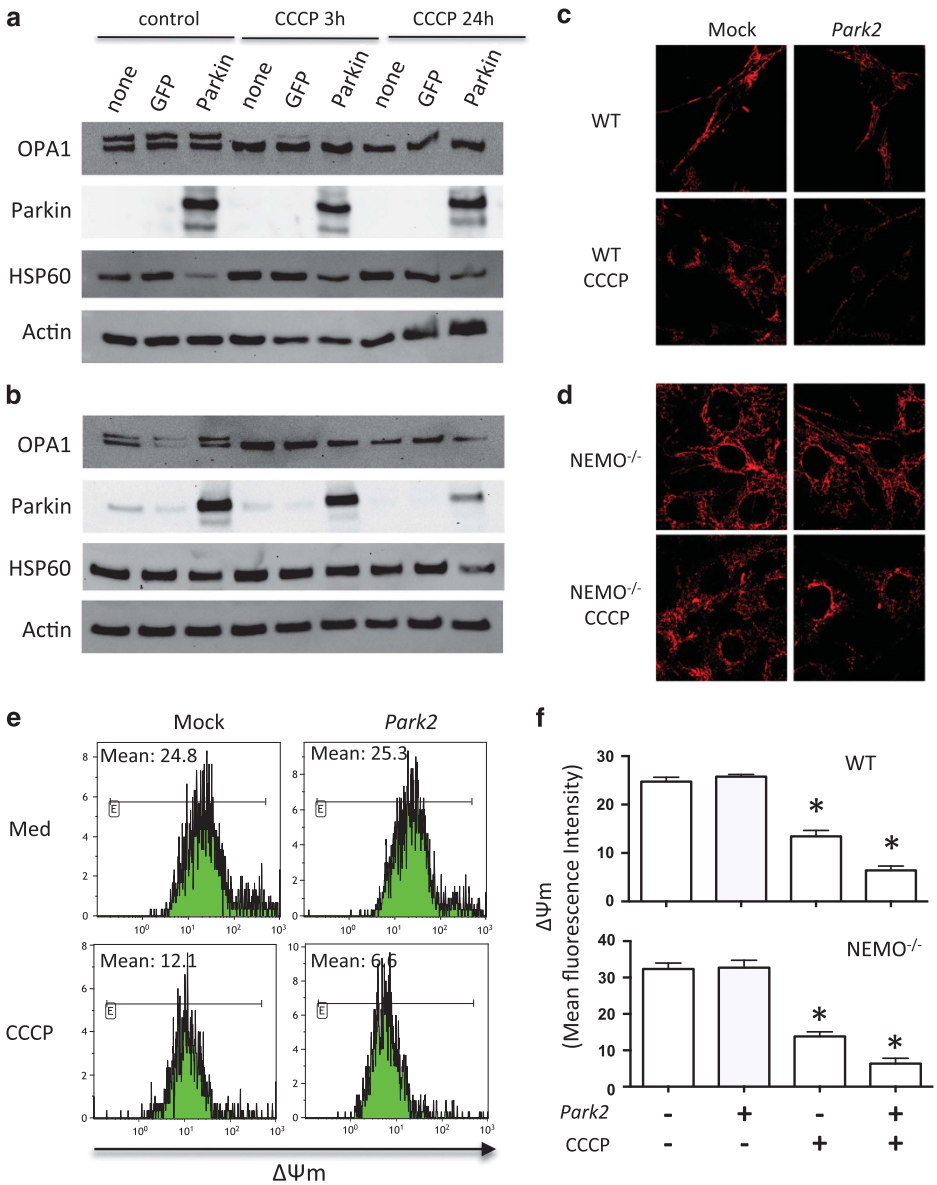

Figure 3 Park2 overexpression in stressed MEF cells. (**a**) Profile of OPA1 expression in WT and (**b**) NEMO$^{-/-}$ MEFs. Cells were transfected with Park2 at a dose of 1 μg. OPA1 expression was assessed at 3 and 24 h in the absence or presence of CCCP. Hsp60 and actin were used as loading controls to normalize protein content. (**c**) WT and (**d**) NEMO$^{-/-}$ MEF cells were stained with specific antibodies directed against Hsp60 (in red). Mitochondrial network was analyzed after overexpression of Park2 in the absence or presence of CCCP after 24 h. (**e**) Mitochondrial membrane potential of WT MEF cells assessed by flow cytometry in the absence or presence of CCCP. (**f**) Histograms of $\Delta\Psi$m from WT and NEMO$^{-/-}$ MEF cells (mean fluorescence intensity) of transfected Park2 cells in the absence or presence of CCCP. Mean $\pm$ SD of three independent experiments; *$P<0.05$

proteasome-dependent degradation. An alternative nonclassical pathway depends on IKK*α* and NF-*κ*B-inducing kinase. Our results showed that, in contrast to NEMO-deficient cells (Figure 1), the amount of long and short isoforms of OPA1 was drastically decreased in IKK*α*- and IKK*αβ*-deficient MEFs but not in IKK*β*-deficient MEFs (Figures 4a and b). In addition, IKK*α*- and IKK*αβ*-deficient MEFs displayed a fragmented mitochondrial network (Figures 4c and d), in the absence of OMM permeabilization, as judged by cytochrome *c* release (Figures 4c and d). Furthermore, we demonstrated in both IKK*α*- and IKK*αβ*-deficient MEFs that mitochondrial network is recovered (Figures 5a and b) and OPA1 expression (Figures 5c and d) after the overexpression of IKK*α* but not after IKK*β* or NEMO expressions.

To gain further insight into the role of Parkin in the regulation of OPA1 expression through the classical and nonclassical NF-kB pathways, we analyzed the impact of *PARK2* overexpression in MEFs deficient for either IKK*α*, IKK*β*, or both.[14] Our western blot results showed that, in none of the MEFs tested, transfection with the *PARK2* vector, at a dose of 0.5 or 1 μg, did significantly increase the amount of OPA1 normalized to mitochondrial HSP60 levels (Figures 6a–c). Furthermore, we did not observe major changes in OPA1 mRNA expression by RT-PCR after transfection with the *PARK2* vector compared

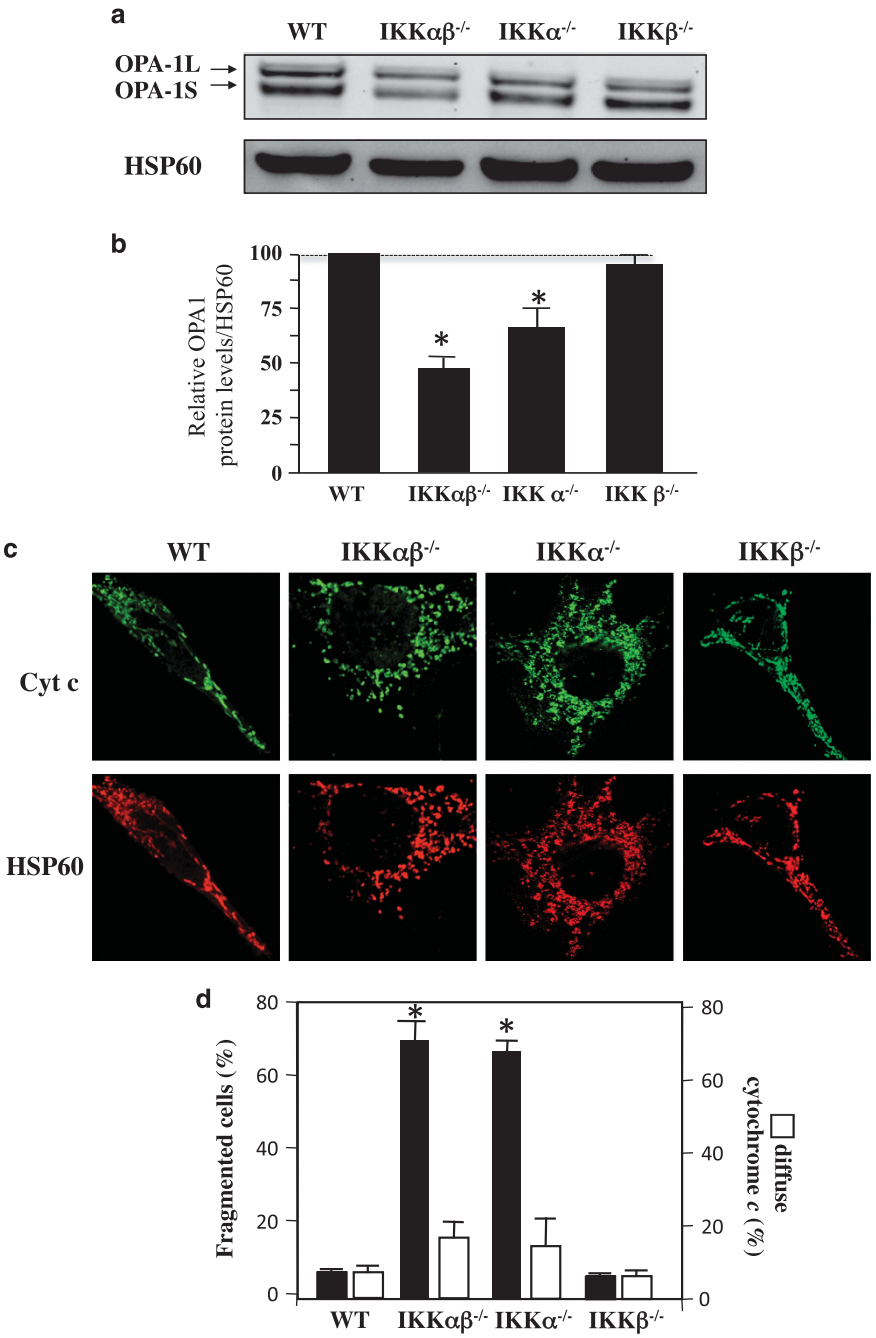

Figure 4 Mitochondrial fragmentation and OPA1 loss in IKKα- and IKK$\alpha\beta$-deficient MEFs. (**a**) OPA1 profile in WT, IKK$\alpha\beta^{-/-}$, IKK$\alpha^{-/-}$, and IKK$\beta^{-/-}$ MEFs. Immunoblot was probed with specific OPA1 antibodies. Hsp60 was used as loading control to normalize protein content. (**b**) Results correspond to the mean of three experiments. *$P<0.05$ compared with WT and IKK$\beta^{-/-}$ MEF cells. (**c**) WT and in IKK$\alpha\beta^{-/-}$ and IKK$\alpha^{-/-}$ cells were stained with specific antibodies directed against cytochrome *c* (Cyt *c*, in green) and HSP60 (in red). (**d**) The histograms show the percentage of cells displaying mitochondrial fragmentation (% fragmented mitochondria) and the release and disappearance of cytochrome *c* (% diffuse Cyt c). For each condition, 150 cells were analyzed. Mean ± S.D. of three independent experiments; *$P<0.05$

with the GFP vector alone in all the MEFs tested (Figure 6d). Therefore, by using different cell lines, we excluded an impact of cell culture conditions on the absence of Parkin effect on OPA1 expression. Thus, overexpression of Parkin appeared to have a minor role in regulating OPA1 expression in MEF cells. This is in agreement with a previous report,[6] in which the overexpression of Parkin in Hela cells was not associated with an increase in the amount of OPA1.

Overexpression of Park2 reduces Bax expression and cell death. To delineate the role of Parkin in apoptosis, we analyzed the effect of its overproduction in the different MEF lines on the expression of two proapoptotic molecules with a crucial role in the control of mitochondria permeabilization, Bax, and Bak.[24] Our results revealed that, at the dose of 1 μg of *PARK2* vector, the amount of Bax normalized to actin was lower in WT, Parkin-deficient, and IKK$\alpha\beta$-deficient MEFs than

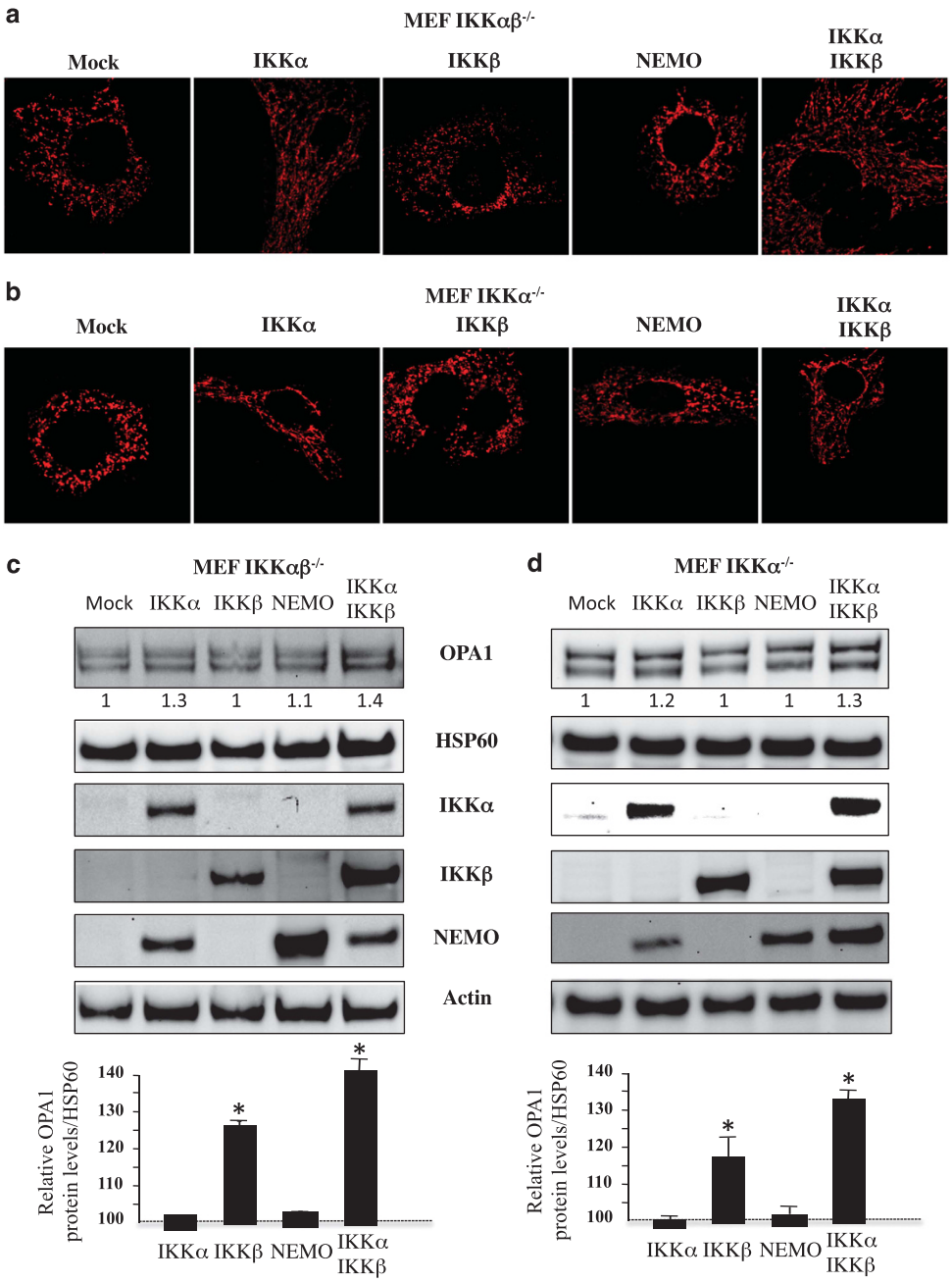

Figure 5 Mitochondrial network fragmentation and OPA1 expression. (**a**, **c**) IKK$\alpha\beta^{-/-}$ and (**b**, **d**) IKK$\alpha^{-/-}$ MEF cells were transfected with plasmids encoding for IKKα, IKKβ, NEMO, or both IKKα+IKKβ at the dose of 1 μg, mock serves as a control. (**a** and **b**) After overnight culture, cells were stained with specific antibodies directed against HSP60 (in red) and mitochondrial fragmentation was analyzed (**c** and **d**) OPA1 expression. As control Hsp60 was used as loading control to normalize protein content. Furthermore immunoblots were probed with specific antibodies to IKKα, IKKβ, and NEMO. Actin was used as a control. Mean $\pm$ S.D. of three independent experiments; *$P<0.05$

in nontransfected cells or in cells transfected with a GFP vector (Figures 7a and c). We did not observe differences in the amount of Bak in any of the cell lines following overexpression of Parkin.

Finally, we assessed whether the ectopic expression of Parkin protected WT or *PARK2*-deficient MEFs from cell death induced by staurosporine (STS) (Figure 8). Ectopic expression of Parkin in MEF cells had no protective effect against STS-mediated cell death in WT (Figures 8a and b) or in Parkin-deficient MEFs (Figure 8c). Because in MEF cells Bax and Bak are functionally redundant in regulating apoptosis,[25] the reduction in the amount of Bax is probably not sufficient to provide protection in these conditions. These results are consistent with an early report showing that Parkin had a minor effect on a large panel of apoptotic stimuli including STS.[26] The protective effect of Parkin observed in neuronal cells by Johnson *et al*. in similar conditions[27] probably reflects the fact that Bax is essential to prevent death in neurons, whereas Bak has no role.[28,29] Therefore, we assessed *PARK2* overexpression in Bak-deficient MEF cells (Figures 8d and e). In this

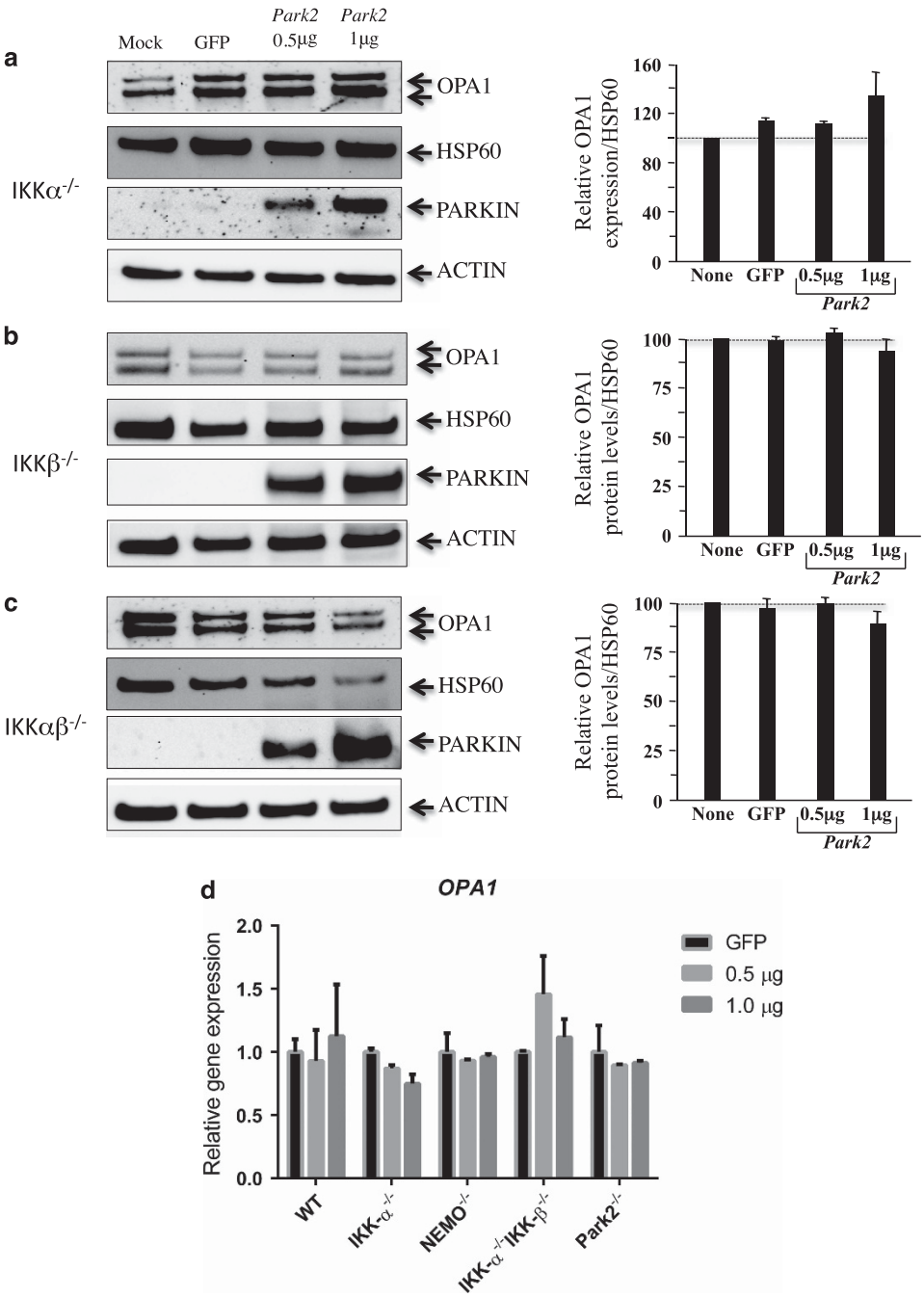

Figure 6 OPA1 expression in Parkin-transfected MEF cells. (**a**) IKK$\alpha^{-/-}$, (**b**) IKK$\beta^{-/-}$, and (**c**) IKK$\alpha\beta^{-/-}$. MEFs were cotransfected with vectors encoding *PARK2*, GFP, or mock. The values indicate the relative levels of the long isoforms with respect to the baseline (value 1), in the absence (mock) or after 24 h of transfection with either GFP or *PARK2* at the dose of 0.5 and 1 μg. HSP60 was used as a loading control to normalize protein content. Immunoblots were also probed with specific Parkin antibodies. Actin was used as a loading control. Four experiments were performed. (**d**) mRNA expression of OPA1 in Parkin–transfected MEF cells. RT-PCRs were performed in WT, IKK$\alpha^{-/-}$, NEMO$^{-/-}$, IKK$\alpha\beta^{-/-}$, and Parkin$^{-/-}$. The values indicate the relative gene expression of OPA1 with respect to the GFP baseline (value set as 1). Two experiments were performed

context, our results demonstrated a protective effect of Parkin on STS-mediated mitochondrial depolarization (Figure 8d) and cell death (Figure 8e). This effect was not dependent on the dose used, as in a recent report the authors show that at the dose of 20 μg, which is 20-fold higher than the dose used here, *Park2* overexpression favors cell death.[30]

Conclusions

In conclusion, our results demonstrate that despite a decrease in the level of OPA1, associated with reductions in mitochondrial network in Parkin-deficient cells, *PARK2* overexpression had no impact on the expression of OPA1 in MEF cells. Thus, these findings do not confirm the major role of Parkin in OPA1

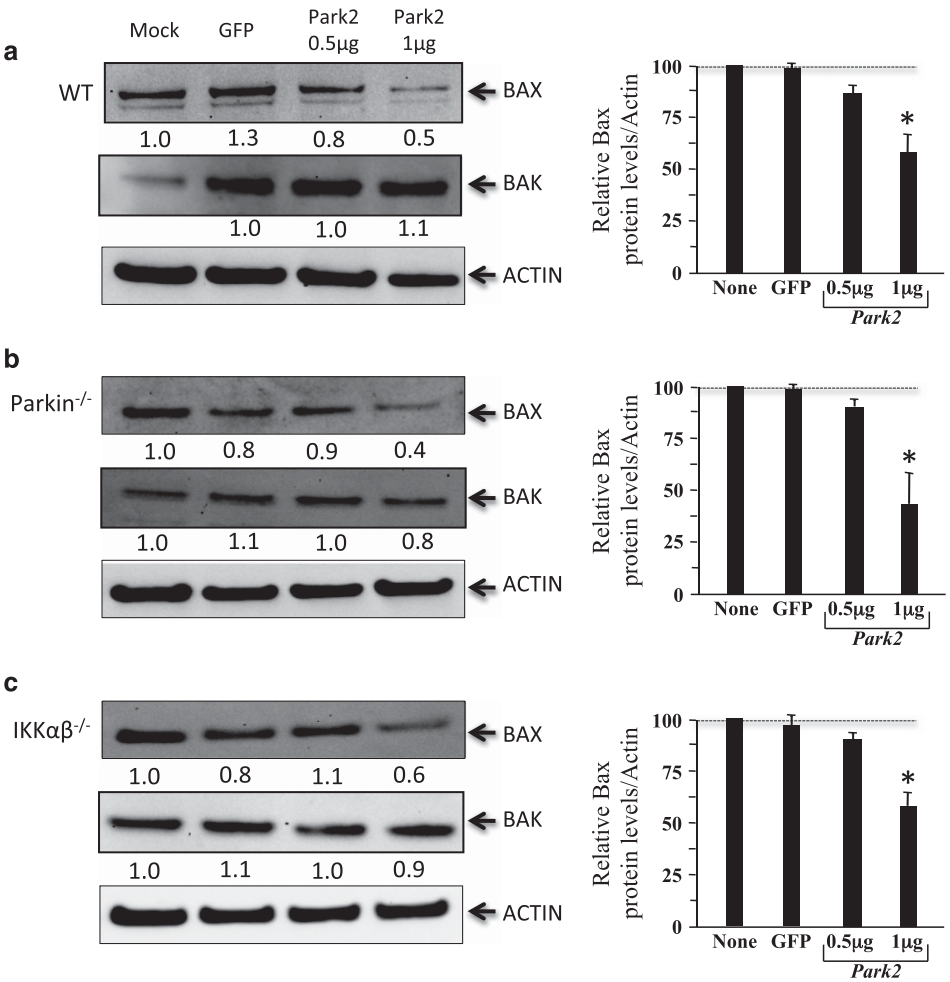

Figure 7 Modulation of Bax and Bak expressions in Parkin-transfected MEF cells. Immunoblots from (**a**) WT, (**b**) Parkin$^{-/-}$ and (**c**) Ikk$\alpha\beta^{-/-}$ as described in Figure 2 and Figure 6 were probed with Bax and Bak antibodies. Values indicate Bax and Bak levels with respect to the baseline (mock, value set as 1) and to actin as a control of loading. Histograms represent mean ± S.D. of three independent experiments; *$P < 0.05$

regulation reported by Müller–Rischart.[13] As Bax has a preponderant role over Bak in primary neurons, the protective effect of Parkin may rather be related to the ubiquitination of Bax and the limitation of its mitochondrial translocation to the mitochondria, previously reported to dampen the apoptotic response.[31] By showing that the absence of IKK*α*, with or without IKK*β*, has an impact on mitochondrial network morphology and OPA1 expression, our results point out a role of the nonclassical NF-κB pathway in the regulation of mitochondrial dynamics and OPA1 expression, rather than to a role of NEMO, which is essential for the canonical NF-κB pathway.

Materials and Methods

Cell culture and reagents. MEF (WT, NEMO$^{-/-}$, IKK$\alpha^{-/-}$, IKK$\beta^{-/-}$, IKK$\alpha\beta^{-/-}$, and Parkin$^{-/-}$) cells were cultured in Dulbecco's modified Eagle's medium (DMEM; Invitrogen, Carlsbad, NM, USA), supplemented with 10% fetal calf serum, 2 mM L-glutamine, 50 IU penicillin, and 50 μg/ml streptomycin in 5% CO_2, at 37 °C. MEF cells were transfected using lipofectamine2000 (Invitrogen) with plasmids encoding for either GFP or PARK2 plasmid. STS was purchased from Sigma (La Chapelle-sur-Erdre, France).

Flow cytometry. After 24 h, Parkin-transfected cells were treated overnight with STS. Cells were also cotransfected with GFP, and the percentage of dying cells was assessed using a propidium iodide nuclear probe (PI^+, Molecular Probes, Life Technology, Cergy Pontoise, France). Mitochondrial membrane potential was assessed using $DioC_6$ (Molecular Probes). Cells were analyzed by flow cytometry (FC500 flow cytometer, Beckman Coulter, Villepinte, France).

Real-time PCR analysis. Total RNA was isolated from the different MEF cell lines after 24 h of transfection. cDNA synthesis was performed using the AffinityScript QPCR cDNA Synthesis Kit (Stratagene, Agilent Technologies, Paris, France) with 1 μg of total RNA and random primers. The resulting complementary-DNA product was expanded using the Absolute Blue QPCR SYBR Green ROX Mix (Thermo Scientific, Illkirch, France) with specific primers for murine *OPA1* (forward: 5′-ACCACAGGAAGCTCAAGAAATC-3′, reverse: 5′-TCTGATCTCCAACCACAAC AAC-3′). Sample input was normalized through quantification of the transcript levels of the housekeeping genes *Gapdh* (forward: 5′- GGCTCATGACCACAGTCC -3′, reverse: 5′-GCAGGGATGATGTTCTGG-3′) and *Rps18* (forward: 5′-GGAAG TACAGCCAGGTTCTG-3′, reverse: 5′-GTGGTCTTGGTGTGCTGAC-3′). Detection was performed with the ABI PRISM 7900HT Sequence Detection System (Applied Biosystems, Saint Aubin, France). Threshold cycle (Ct) values were obtained for each gene using the instrument software and auto-Ct function. The relative levels of gene expression were determined using the delta–delta Ct method.

Immunoblotting. Total lysates were extracted using 1% NP40 (150 mM NaCl, 50 mM Tris HCl pH 7.4, 10 mM EDTA) supplemented by a cocktail of antiproteases and antiphosphatases. A total of 20 μg of proteins from each point were resolved by SDS-NuPAGE (4–12% Bis-Tris gels, Novex, Les Ulis, France) and transferred to

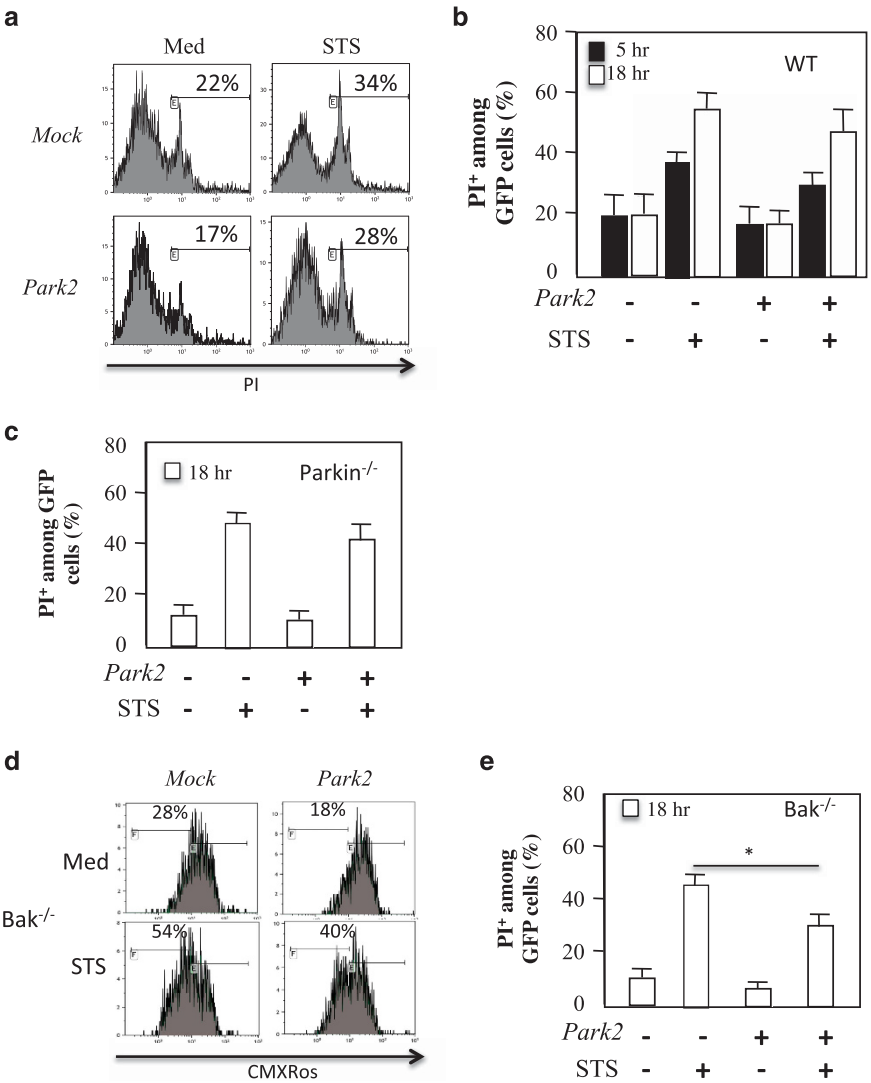

Figure 8 Ovexpression of Park2 prevents cell death in Bak-deficient MEF cells. (**a**) Flow cytometry of WT MEF cells transfected with vectors encoding for *PARK2* and GFP. Cells were treated or not with STS, 500 nM. Cells were gated on GFP and PI staining is shown. Percentage of dying (**b**) WT and (**c**) Parkin$^{-/-}$ MEF cells was analyzed at 5 and 18 h after STS treatment. (**d**) Flow cytometry of Bak$^{-/-}$ MEF cells transfected with vectors encoding for *PARK2* and treated with Staurosporine (STS, 500 nM). Cells were stained with CMXRos. Mitochondrial depolarization is shown. (**e**) Percentage of dying Bak-deficient MEF cells is shown. Histograms represent mean ± S.D. of three independent experiments; $^{*}P<0.05$

nitrocellulose membranes (Amersham Biosciences, Les Ulis, France). Nonspecific sites were blocked by incubation with 5% milk for 1 h at room temperature, and the membranes were then incubated with mouse monoclonal anti-OPA1 (BD Biosciences Pharmingen, Le Pont de Claix, France; clone 18), anti-Parkin (Millipore, Le Pont de Claix, France), and rabbit anti-Bax (N-20, from Santa-Cruz, Le Pont de Claix, France). Antibodies specific for IKKα, IKKβ, and NEMO were purchased from Cell Signaling (St Quentin Fallavier, France). Equal protein loading was assessed by probing the membranes with anti-actin (Millipore) and anti-HSP60 monoclonal antibodies (Stressgen, St Quentin Fallavier, France). Membranes were treated with horseradish peroxidase-linked goat anti-mouse or anti-rabbit secondary antibodies (Amersham Biosciences). Immunoreactive proteins were detected and quantified by enhanced chemiluminescence (Amersham Biosciences) using a CCD camera (GBOX, SYNGENE, Ozyme, France).

Fluorescence microscopy. MEF cells were grown on coverslips and fixed with 4% paraformaldehyde (Sigma-Aldrich, St Quentin Fallavier, France). Cells were incubated for 1 h in blocking buffer (2% bovine serum albumin in phosphate-buffered saline) and then overnight with a mouse monoclonal anti-cytochrome *c* (BD Biosciences, St Quentin Fallavier, France; clone 6H2.B4), or goat anti-HSP60 (Santa Cruz) antibody. Cells were washed and incubated for 2 h with Alexa Fluor secondary anti-mouse, anti-rabbit, or anti-goat antibodies (Molecular Probes). Images were acquired with a Zeiss LSM 510 confocal microscope equipped with an oil-immersion fluorescence objective (Carl Zeiss, Inc., Périgny, France). Cells were also stained with 100 nM Mitotracker green (Invitrogen) for 30 min. Cells were imaged by epifluorescence using a Zeiss Axiovert 200 M inverted microscope. Images were then analyzed using the imageJ software (NIH, Bethesda, MD, USA). Deconvolution was performed by subtracting a Gaussian blur (σ: 12) to the original image. Deconvolved images were then processed with a certain threshold to obtain a binary image of the mitochondrial network. The binary image was then analyzed using the Analyze Particle function of ImageJ to determine the number and the size of mitochondria in individual cells.

Conflict of Interest

The authors declare no conflict of interest.

Acknowledgements. This work was funded by grants to JE from the Agence Nationale de Recherches sur le Sida et les Hépatites Virales (ANRS), the Association

pour la Recherche sur le Cancer (ARC), La Ligue contre le Cancer (Ligue), and the Fondation pour la Recherche Médicale; OC is supported by the Fondation ICM, 'Investissements d'avenir' ANR-10-IAIHU-06. ML is supported by fellowships from the ANRS. VR is supported by a fellowship from FCT code SFRH/BD/64064/2009. We thank C Soundaramourty for her help, and V Baud who kindly provided the IκB kinase-α-deficient MEF cells IKK$\beta^{-/-}$, and IKK$\alpha\beta^{-/-}$. MEF cells were provided by Inder M. Verma, and NEMO MEFs cells were a gift from Marc Schmidt-Supprian. JE acknowledges the support of the Canada Research Chair program.

1. Narendra D, Tanaka A, Suen DF, Youle RJ. Parkin-induced mitophagy in the pathogenesis of Parkinson disease. *Autophagy* 2009; **5**: 706–708.
2. Cherra 3rd SJ , Dagda RK, Tandon A, Chu CT. Mitochondrial autophagy as a compensatory response to PINK1 deficiency. *Autophagy* 2009; **5**: 1213–1214.
3. Vives-Bauza C, Zhou C, Huang Y, Cui M, de Vries RL, Kim J *et al.* PINK1-dependent recruitment of Parkin to mitochondria in mitophagy. *Proc Natl Acad Sci USA* 2010; **107**: 378–383.
4. Matsuda N, Sato S, Shiba K, Okatsu K, Saisho K, Gautier CA *et al.* PINK1 stabilized by mitochondrial depolarization recruits Parkin to damaged mitochondria and activates latent Parkin for mitophagy. *J Cell Biol* 2010; **189**: 211–221.
5. Chen H, Detmer SA, Ewald AJ, Griffin EE, Fraser SE, Chan DC. Mitofusins Mfn1 and Mfn2 coordinately regulate mitochondrial fusion and are essential for embryonic development. *J Cell Biol* 2003; **160**: 189–200.
6. Tanaka A, Cleland MM, Xu S, Narendra DP, Suen DF, Karbowski M *et al.* Proteasome and p97 mediate mitophagy and degradation of mitofusins induced by Parkin. *J Cell Biol* 2010; **191**: 1367–1380.
7. Glauser L, Sonnay S, Stafa K, Moore DJ. Parkin promotes the ubiquitination and degradation of the mitochondrial fusion factor mitofusin 1. *J Neurochem* 2011; **118**: 636–645.
8. Gegg ME, Schapira AH. PINK1-parkin-dependent mitophagy involves ubiquitination of mitofusins 1 and 2: implications for Parkinson disease pathogenesis. *Autophagy* 2011; **7**: 243–245.
9. Youle RJ, Karbowski M. Mitochondrial fission in apoptosis. *Nat Rev Mol Cell Biol* 2005; **6**: 657–663.
10. Corti O, Brice A. Mitochondrial quality control turns out to be the principal suspect in parkin and PINK1-related autosomal recessive Parkinson's disease. *Curr Opin Neurobiol* 2013; **23**: 100–108.
11. Henn IH, Bouman L, Schlehe JS, Schlierf A, Schramm JE, Wegener E *et al.* Parkin mediates neuroprotection through activation of IkappaB kinase/nuclear factor-kappaB signaling. *J Neurosci* 2007; **27**: 1868–1878.
12. Sha D, Chin LS, Li L. Phosphorylation of parkin by Parkinson disease-linked kinase PINK1 activates parkin E3 ligase function and NF-kappaB signaling. *Hum Mol Genet* 2010; **19**: 352–363.
13. Muller-Rischart AK, Pilsl A, Beaudette P, Patra M, Hadian K, Funke M *et al. Mol Cell* 2013; **49**: 908–921.
14. Israel A. The IKK complex, a central regulator of NF-kappaB activation. *Cold Spring Harb Perspect Biol* 2010; **2**: a000158.
15. Cipolat S, Rudka T, Hartmann D, Costa V, Serneels L, Craessaerts K *et al.* Mitochondrial rhomboid PARL regulates cytochrome c release during apoptosis via OPA1-dependent cristae remodeling. *Cell* 2006; **126**: 163–175.
16. Frezza C, Cipolat S, Martins de Brito O, Micaroni M, Beznoussenko GV, Rudka T *et al.* OPA1 controls apoptotic cristae remodeling independently from mitochondrial fusion. *Cell* 2006; **126**: 177–189.
17. Estaquier J, Vallette F, Vayssiere JL, Mignotte B. The mitochondrial pathways of apoptosis. *Adv Exp Med Biol* 2012; **942**: 157–183.
18. Olichon A, Baricault L, Gas N, Guillou E, Valette A, Belenguer P *et al.* Loss of OPA1 perturbates the mitochondrial inner membrane structure and integrity, leading to cytochrome c release and apoptosis. *J Biol Chem* 2003; **278**: 7743–7746.
19. Arnoult D, Grodet A, Lee YJ, Estaquier J, Blackstone C. Release of OPA1 during apoptosis participates in the rapid and complete release of cytochrome c and subsequent mitochondrial fragmentation. *J Biol Chem* 2005; **280**: 35742–35750.
20. Duvezin-Caubet S, Koppen M, Wagener J, Zick M, Israel L, Bernacchia A *et al.* OPA1 processing reconstituted in yeast depends on the subunit composition of the m-AAA protease in mitochondria. *Mol Biol Cell* 2007; **18**: 3582–3590.
21. Mortiboys H, Thomas KJ, Koopman WJ, Klaffke S, Abou-Sleiman P, Olpin S *et al.* Mitochondrial function and morphology are impaired in parkin-mutant fibroblasts. *Ann Neurol* 2008; **64**: 555–565.
22. Grunewald A, Voges L, Rakovic A, Kasten M, Vandebona H, Hemmelmann C *et al.* Mutant Parkin impairs mitochondrial function and morphology in human fibroblasts. *PloS One* 2010; **5**: e12962.
23. Lutz AK, Exner N, Fett ME, Schlehe JS, Kloos K, Lämmermann K *et al.* Loss of parkin or PINK1 function increases Drp1-dependent mitochondrial fragmentation. *J Biol Chem* 2009; **284**: 22938–22951.
24. Tait SW, Green DR. Mitochondria and cell death: outer membrane permeabilization and beyond. *Nat Rev Mol Cell Biol* 2010; **11**: 621–632.
25. Wei MC, Zong WX, Cheng EH, Lindsten T, Panoutsakopoulou V, Ross AJ *et al.* Proapoptotic BAX and BAK: a requisite gateway to mitochondrial dysfunction and death. *Science* 2001; **292**: 727–730.
26. Darios F, Corti O, Lücking CB, Hampe C, Muriel MP, Abbas N *et al.* Parkin prevents mitochondrial swelling and cytochrome c release in mitochondria-dependent cell death. *Hum Mol Genet* 2003; **12**: 517–526.
27. Johnson BN, Berger AK, Cortese GP, Lavoie MJ. The ubiquitin E3 ligase parkin regulates the proapoptotic function of Bax. *Proc Natl Acad Sci Usa* 2012; **109**: 6283–6288.
28. Putcha GV, Harris CA, Moulder KL, Easton RM, Thompson CB, Johnson Jr EM . Intrinsic and extrinsic pathway signaling during neuronal apoptosis: lessons from the analysis of mutant mice. *J Cell Biol* 2002; **157**: 441–453.
29. Deckwerth TL, Elliott JL, Knudson CM, Johnson Jr EM, Snider WD, Korsmeyer SJ. BAX is required for neuronal death after trophic factor deprivation and during development. *Neuron* 1996; **17**: 401–411.
30. Carroll RG, Hollville E, Martin SJ. Parkin sensitizes toward apoptosis induced by mitochondrial depolarization through promoting degradation of Mcl-1. *Cell Rep* 2014; **9**: 1538–1553.
31. Easton RM, Deckwerth TL, Parsadanian AS, Johnson Jr EM. Analysis of the mechanism of loss of trophic factor dependence associated with neuronal maturation: a phenotype indistinguishable from Bax deletion. *J Neurosci* 1997; **17**: 9656–9666.